Supporting Information

Multifunctional theranostic nanoparticles for multi-model imaging-guided CAR-T immunotherapy, chemo-photothermal combinational therapy of non-Hodgkin's lymphoma

Bowen Shi,‡[a] Dan Li,‡[b] Weiwu Yao,‡[c] Wenfang Wang,[a] Jiang Jiang,[a] Ruiheng Wang,[b] Fuhua Yan,[a] Han Liu,*[b] Huan Zhang*[b] and Jian Ye*[d,e]

[a] Department of Radiology, Ruijin Hospital Affiliated to Shanghai Jiao Tong University School of Medicine, Shanghai 200025, P. R. China. E-mail: zh10765@rjh.com.cn

[b] Shanghai Institute of Hematology, State Key Laboratory of Medical Genomics, National Research Center for Translational Medicine at Shanghai, Ruijin Hospital Affiliated to Shanghai Jiao Tong University School of Medicine, Shanghai 200025, P. R. China. E-mail: liuhan68@sjtu.edu.cn

[c] Department of Radiology, Tongren Hospital Affiliated to Shanghai Jiao Tong University School of Medicine, Shanghai 200050, P. R. China

[d] School of Biomedical Engineering, Shanghai Jiao Tong University, Shanghai 200030, P. R. China. E-mail: yejian78@sjtu.edu.cn

[e] Institute of Medical Robotics, Shanghai Jiao Tong University, Shanghai 200240, P. R. China

* Corresponding authors.

E-mail addresses: liuhan68@sjtu.edu.cn (H. Liu), zh10765@rjh.com.cn (H. Zhang), yejian78@sjtu.edu.cn (J. Ye).

‡These authors contributed equally to this work.

Supplementary experimental section

Materials

Chloroauric chloride ($HAuCl_4•H_2O$), ascorbic acid, tetraethyl orthosilicate (TEOS) and sodium hydroxide (NaOH) were bought from Sinopharm Chemical Reagent Co. Ltd. Cetyltrimethylam-monium chloride (CTAC), sodium borohydride ($NaBH_4$) and maleimide-PEG-NH_2 were obtained from J&K Chemical Ltd (Shanghai, China). Ibrutinib (PCI-32765) was purchased from Selleckchem (Houston, USA). Maleimide-DOTA was obtained from Macrocyclics. Folic acid (FA), 4-Nitrobenzenethiol (4-NBT), (3-mercaptopropyl) trimethoxysilane (MPTMS), gadolinium chloride ($GdCl_3$), 1-(3-dimethylaminopropyl)-3-ethylcarbodiinide hydrochloride (EDC) and N-hydroxysuccinimide (NHS) were purchased from Sigma-Aldrich (Shanghai, China). 3-(4,5-dimethylthiazol-2-yl) −2,5-diphenyltetrazolium bromide (MTT) was received from S Nanjing Keygen Biotech. Co., Ltd. (Nanjing, China). DMEM/high glucose medium, DMEM/F-12 (Ham) medium, penicillin–streptomycin mixture solution and fetal bovine serum (FBS) were purchased from Gibco Life Technologies (USA). Deionized water (Millipore) with a resistivity of 18 MΩ cm was used for all experiments. All materials were used as received without any further purification.

Characterization

The morphology images of the nanoparticle were investigated on a JEM-2100F transmission electron microscopy (TEM) platform (JEOL, Tokyo, Japan). UV-Vis spectra were obtained on a Shimadzu UV-1900 spectrophotometer (Aucybest, Shanghai, China) at room temperature. And, the surface zeta potential and hydrodynamic size of nanoparticles were evaluated in deionized water, using a Malvern Zetasizer Nano ZS90. The Raman test was carried out on

confocal Raman microscope (Horiba, Xplora INV). Laser irradiation was conducted by the excitation source with a diode-pumped solid-state laser system (Laserglow Technologies, Shanghai, China).

***In vitro* cell cytotoxicity assessment**

JEKO cells and RAJI cells were seeded were seeded in 96-wells plate with a density of 1 × 10^4/well and incubated with the different FA-Gd-GERTs concentrations (0-100 μM) at 37 °C and 5% CO_2 for 24 h. After that, the standard MTT assay was carried out to determine the cell viability. Three replicates were done for each treatment group.

Flow cytometry

The CellTrace Far Red Proliferation Kit, the CellTrace CFSE Cell Proliferation Kit and the CellTrace Violet Proliferation Kit (Invitrogen) were used for cell labeling. The APC anti-human folate receptors antibody was obtained from Biolegend (San Diego, California). Apoptosis was measured using the Annexin V Apoptosis Detection Kit (BD Bioscience). Flow cytometry was performed on LSRFortessa or FACSAria sorter (BD Biosciences). Data were analyzed by the FlowJo software.

***In vitro* CT/MR/SERS imaging**

Approximately 5 × 10^6 JEKO cells and RAJI cells were allowed to seed on the quartz-bottomed plates for 20 h, then incubated with FA-Gd-GERTs or Gd-GERTs (0, 20, 40, 60, 80 and 100 mM, respectively) at 37 °C and 5% CO_2 for 4 h, the cells were trypsinized, centrifuged, resuspended in 1 mL PBS, and placed in 1.5-mL tubes. For CT imaging, the cell suspension in each tube was placed in a self-designed scanning holder and then scanned using a dual-source CT imaging system (Siemens Healthineers, Forchheim Germany) operating at 100 kV, 80 mA,

and a slice thickness of 0.625 mm. The CT values were acquired on the same workstation using the software supplied by the manufacturer. Each experiment was performed in triplicate. For T_1 MR imaging, the T_1 relaxation time for each sample was measured using a 3.0 T clinical MR imaging instrument (Ingenia, Philips Healthcare, Best, The Netherlands) with a wrist receiver coil and a fast spin-echo (FSE) sequence (TR/TE: 2000/81.9 ms, matrix: 256×256, section thickness: 2 mm, and FOV: 80×80 mm).

***In vivo* CT/MR/SERS imaging**

Follow-up CT and MR studies were performed after intravenous injection of the FA-Gd-GERTs (0.2 mL in saline solution, [Au] = 0.05 M). The mice were performed by using a dual-source CT imaging system (Siemens Healthineers, Forchheim Germany) with a tube voltage of 70 kV, an electrical current of 752 mAs, a slice thick- ness of 0.5 mm, and a scan field of view of 45 mm × 80 mm. CT values were acquired on the same workstation using the software supplied by the manufacturer. For MR imaging, a 3.0 T clinical MR imaging instrument (Ingenia, Philips Healthcare, Best, The Netherlands) with a 16-channel human wrist coil was performed. The parameters of the T_1-weighted MRI were used as follows: pulse waiting time (TR), 2800 ms; echo time (TE), 60 ms; and slice width (SW), 5.0 mm. The signal-to-noise ratio was recorded to quantify the T_1-weighted MRI enhancement effect. SERS imaging was performed on a Raman confocal system with 785-nm laser excitation, 10 × objective lens, and 3.7×10^5 W/cm^2 power density. All SERS images were obtained with a Macro mapping mode to minimize the imaging time with an exposure time of 1 s/spectrum, a step size of 500 μm. During the Macro mapping mode, the laser beam is raster-scanned to record an average spectrum across the whole area, and the sample is moved on the motorized stage with a step

matched to the scanned area size to cover the whole surface. All the SERS reconstruction images were generated with the characteristic band of Gd-GERTs at 1335 cm^{-1} by using the LabSpec 6 software.

In vivo infrared thermal imaging

For evaluating the FA-Gd-GERTs@Ibrutinib photothermal effect *in vivo*, we intravenously injected the 200 μL Gd-GERTs@Ibrutinib and FA-Gd-GERTs@Ibrutinib ([Au]=0.05 M) respectively. After 2 h, we irradiated the tumor site with a 0.5 W/cm^2 laser for 5 min and the photothermal images were acquired using the infrared thermal imaging camera.

Statistical analysis

All Data were presented as mean ± SD with at least three repetitive experiments in each group. Student's t-test statistical analysis was performed using statistics software (SPSS v. 22.0; IBM, Armonk, NY).

Supplementary figures

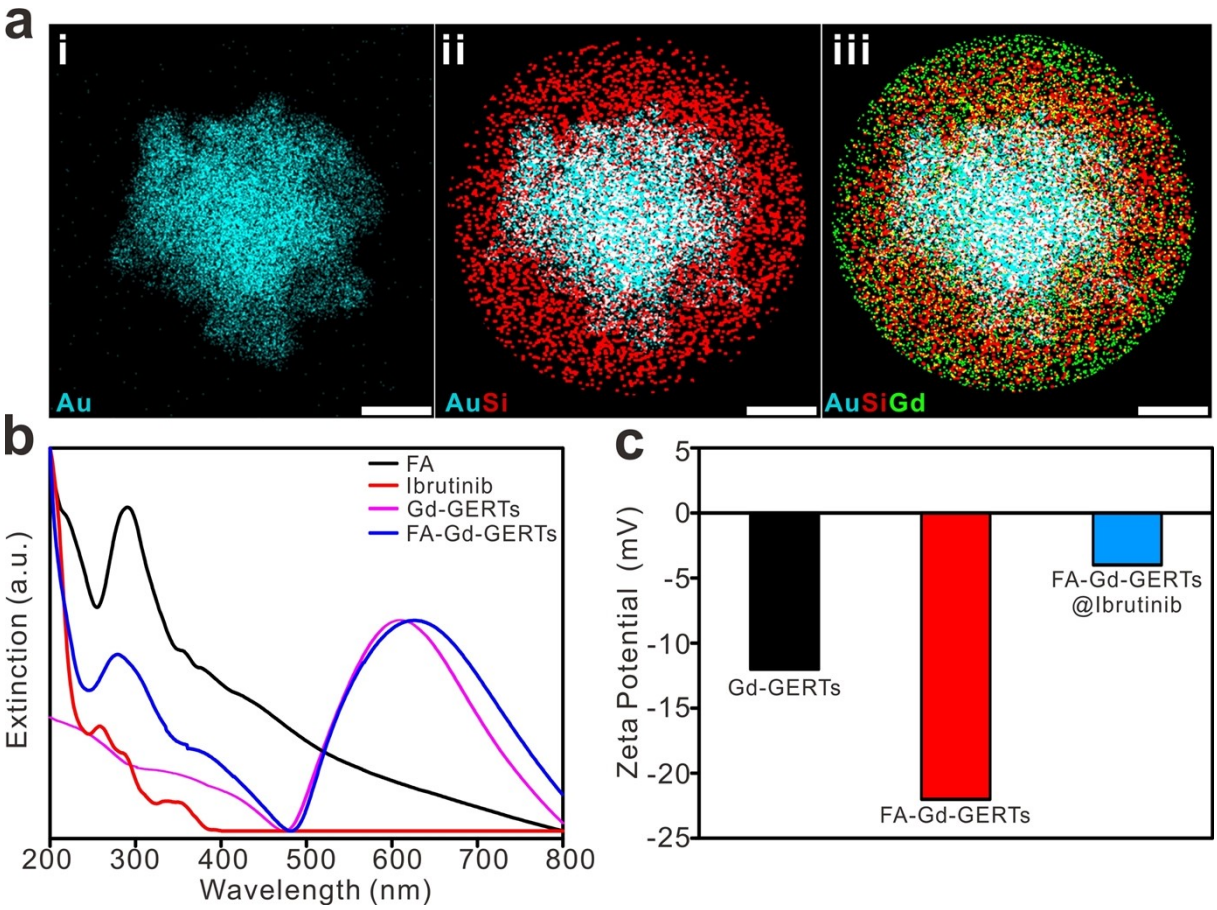

Fig. S1. (a) EDS elemental mapping images of Au, overlay of Si, and overlay of Gd of FA-Gd-GERTs@Ibrutinib. The scale bars are 25nm. (b) UV-vis absorption spectra of Gd-GERTs, FA, ibrutinib, and FA-Gd-GERTs dispersions. (c) Zeta potential of the Gd-GERTs, FA-Gd-GERTs and FA-Gd-GERTs@Ibrutinib.

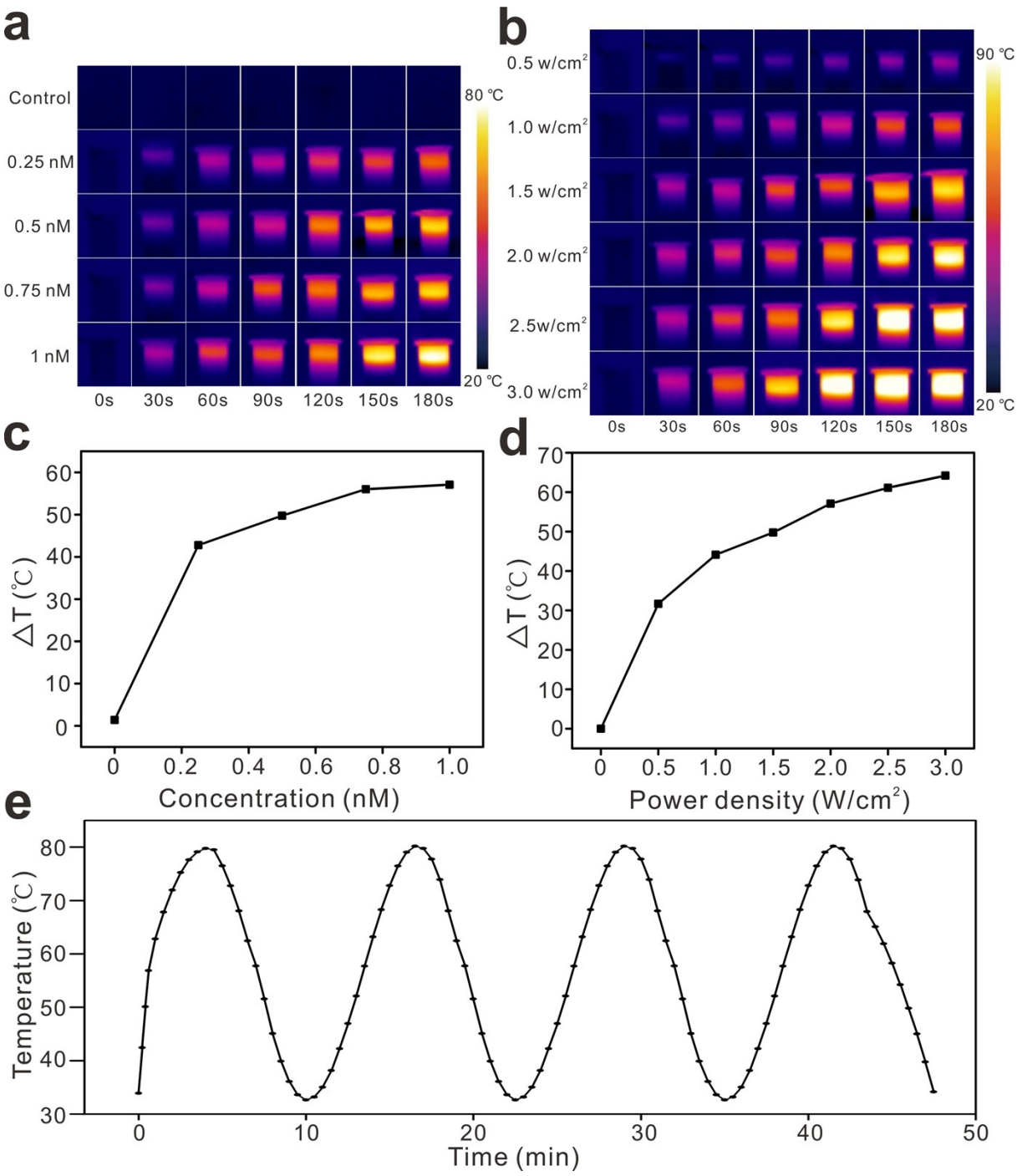

Fig. S2. *In vitro* NIR thermographic images of aqueous FA-Gd-GERTs@Ibrutinib with different concentrations (a) and various laser power densities (b). Plot of temperature change (ΔT) over a period of 3 min versus the particle concentration (c), and the irradiation power density (d). Temperature monitoring of FA-Gd-GERTs@Ibrutinib aqueous suspension during for successive cycles of an on-and-off laser (e).

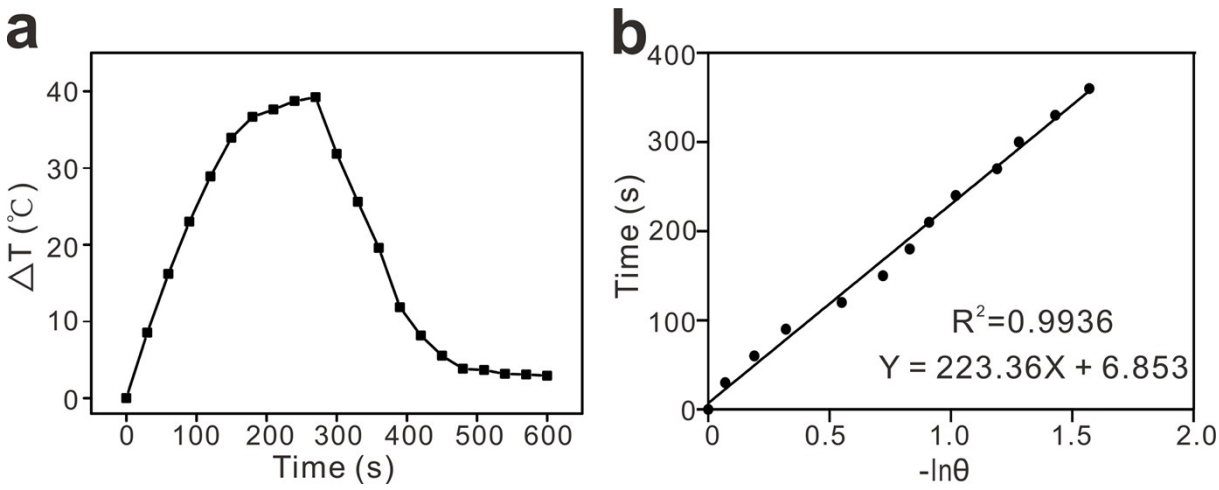

Fig. S3. (a) Temperature change of FA-Gd-GERTs@Ibrutinib during heating and cooling period. (b) The plot of cooling time (t) versus the negative natural logarithm of the temperature driving force (θ) obtained from the cooling stage for evaluating the photothermal conversion efficiency.

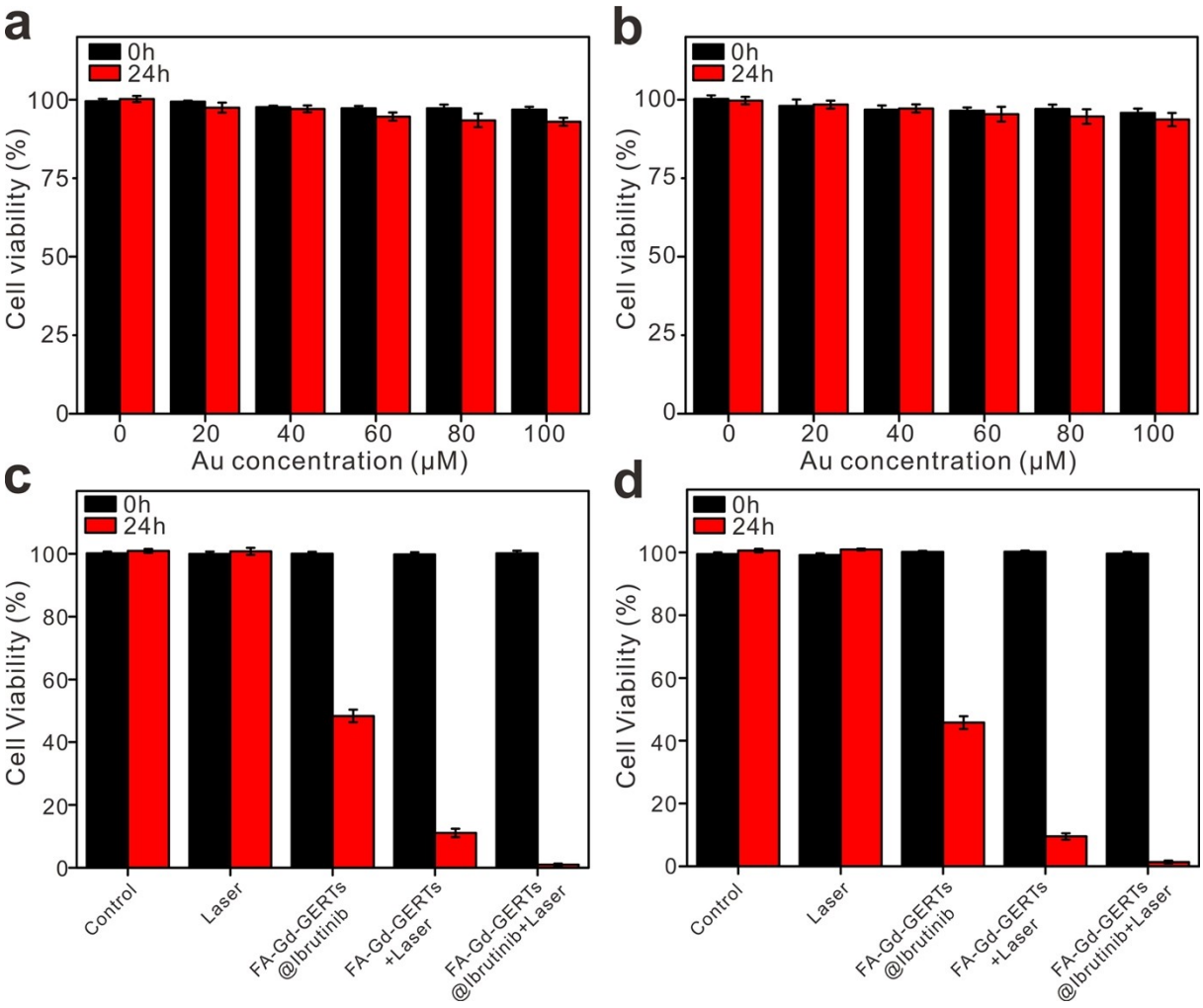

Fig. S4. MTT assay of the viability of JEKO cells (a) and RAJI cells (b) treated with FA-Gd-GERTs at a series of concentrations for 24 h. The cell viability of JEKO cells (c) and RAJI cells (d) treated with different conditions. Data are represented as mean ± standard deviation.

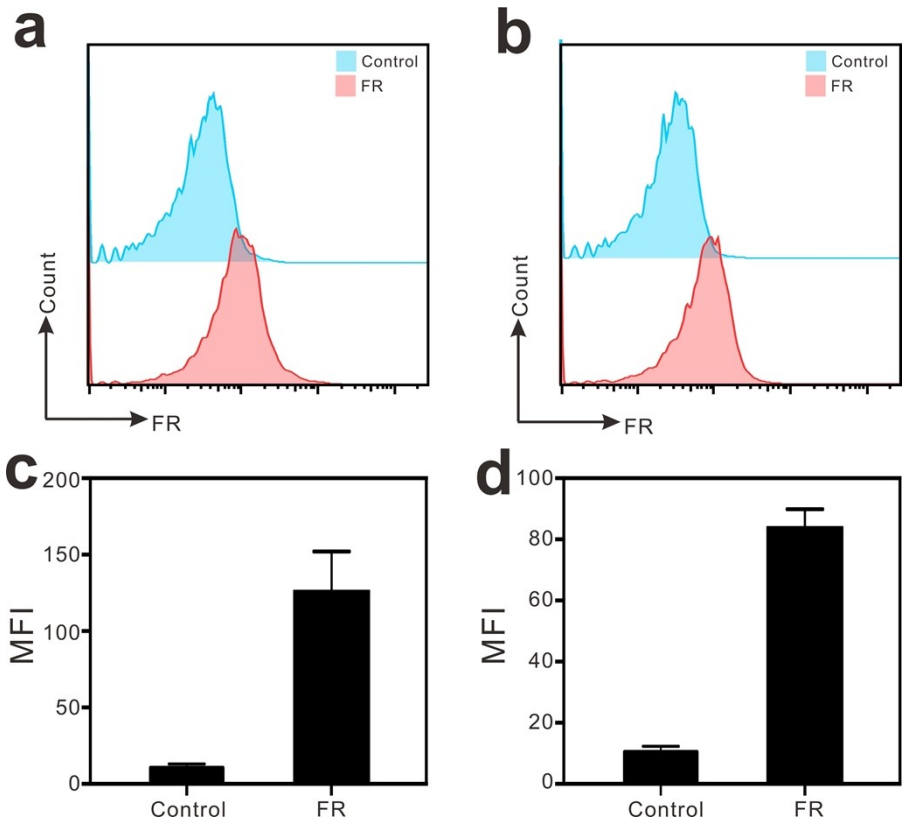

Fig. S5. Flow cytometry analyses of the expression of FR in the JEKO (a) and RAJI cells (b). The mean fluorescence intensity of FR in JEKO (c) and RAJI cells (d), indicating the anti-FR antibody bonding with the tumor cells.

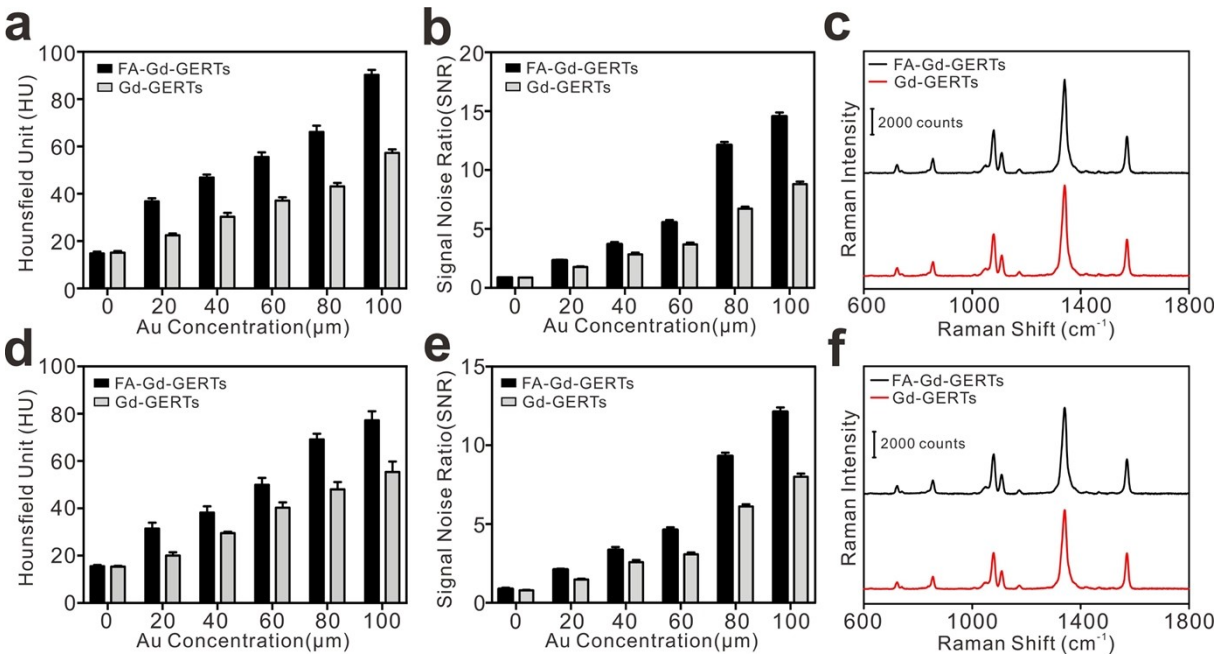

Fig. S6. The CT HU value, MR SNRs and Raman spectra of JEKO cells (a-c) and RAJI cells (d-f) incubated with FA-Gd-GERTs and Gd-GERTs at different Au concentrations for 4 h.

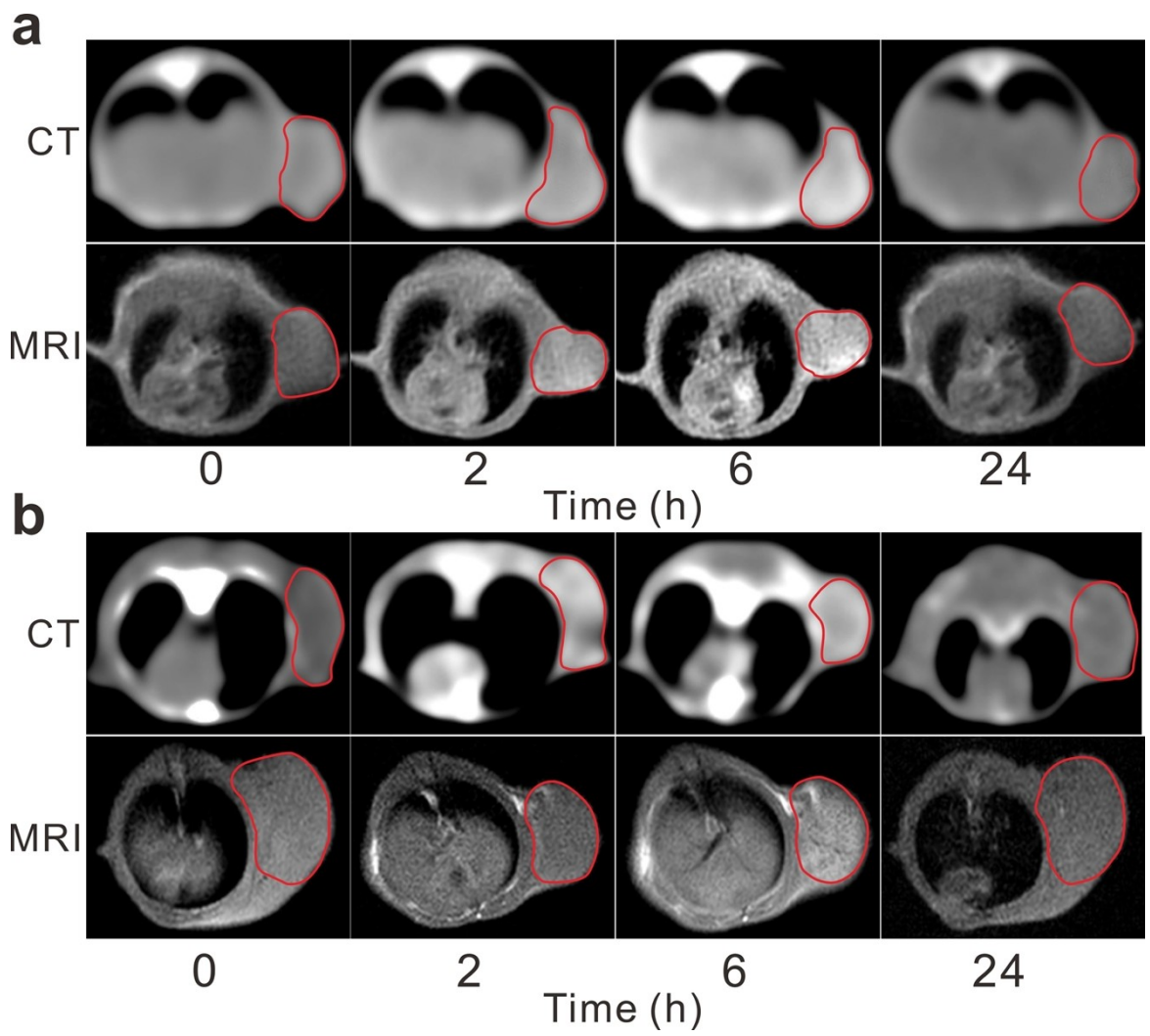

Fig. S7. Representative transection *in vivo* CT and MR images of control group bearing (a) JEKO and (b) RAJI tumors after the intravenous injection of saline at different timepoint. The red circles indicate the tumor areas.

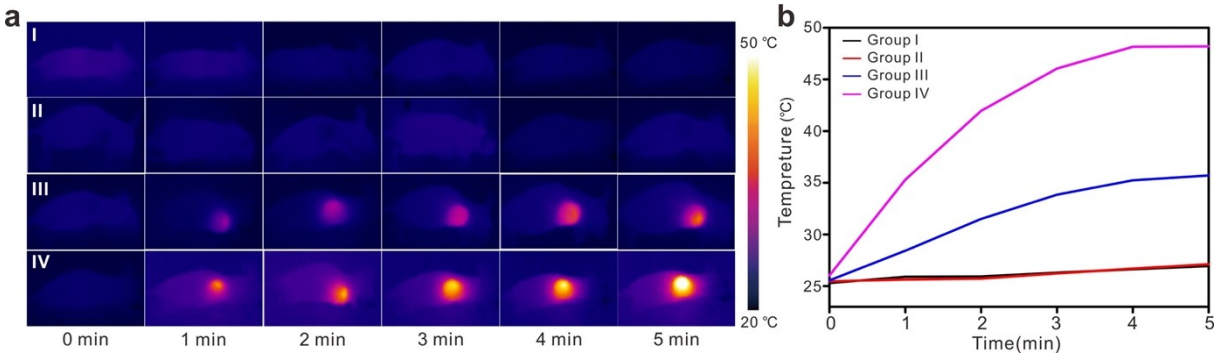

Fig. S8. (a) *In vivo* infrared thermal images JEKO tumor bearing mice and (d) the corresponding temperature increasing curves of saline (Group I), saline with laser (Group II), Gd-GERTs@Ibrutinib with laser irradiation (Group III), and FA-Gd-GERTs@Ibrutinib with laser irradiation (Group IV).

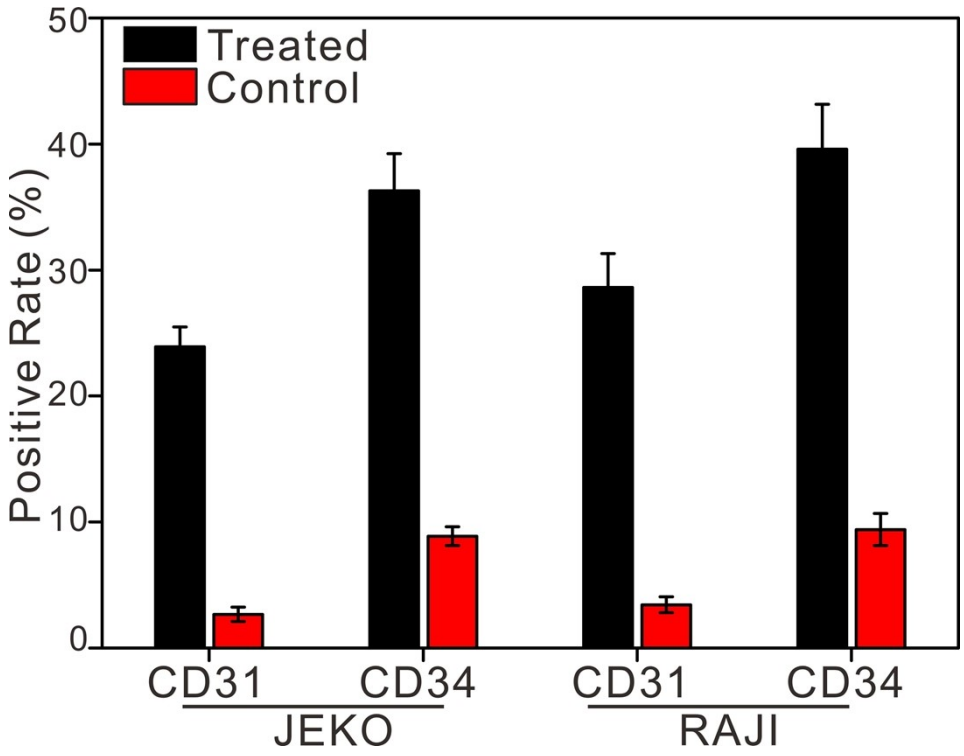

Fig. S9. The positive rates of CD31 and CD34 expression in JEKO and RAJI tumors.

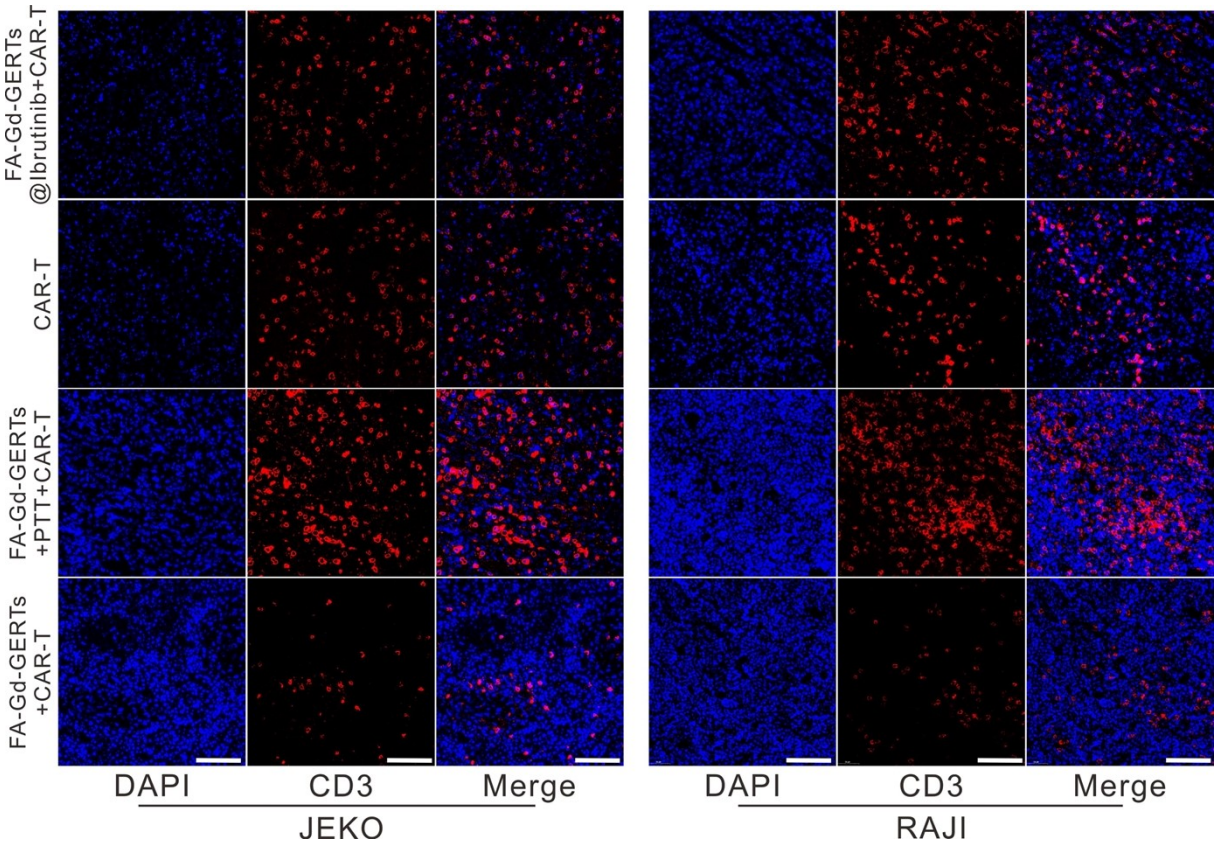

Fig. S10. The representative CD3 T cells immunofluorescence images of JEKO and RAJI tumors after different treatments. The scale bar is 100 μm.

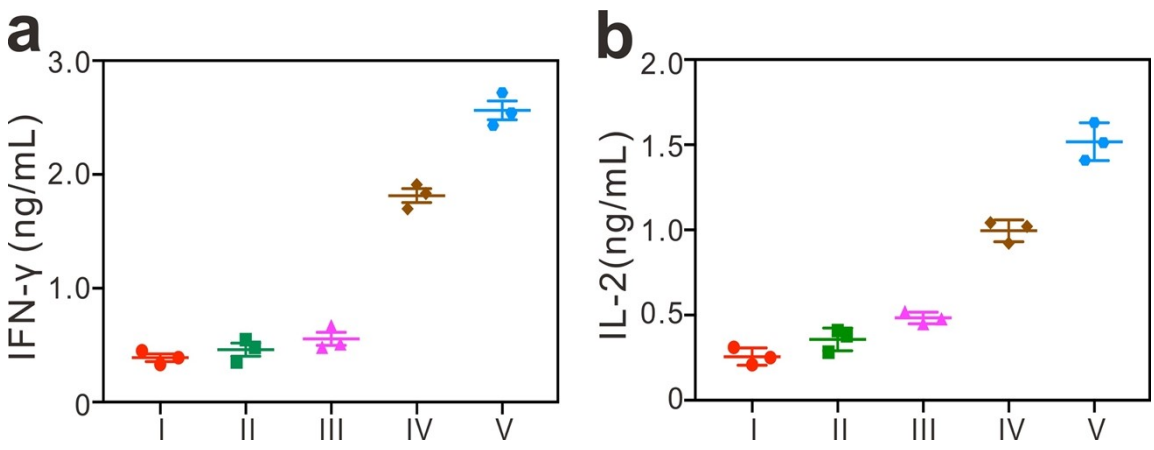

Fig. S11. Human IFN-γ (a) and IL-2 (b) levels detected in the tumors after the different treatments: (I) control; (II) injected FA-Gd-GERTs@Ibrutinib only; (III) FA-Gd-GERTs@Ibrutinib + Laser; (IV) intravenously injected with CD19 CAR-T cells only and (V) FA-Gd-GERTs@Ibrutinib + Laser + CD19 CAR-T cells.

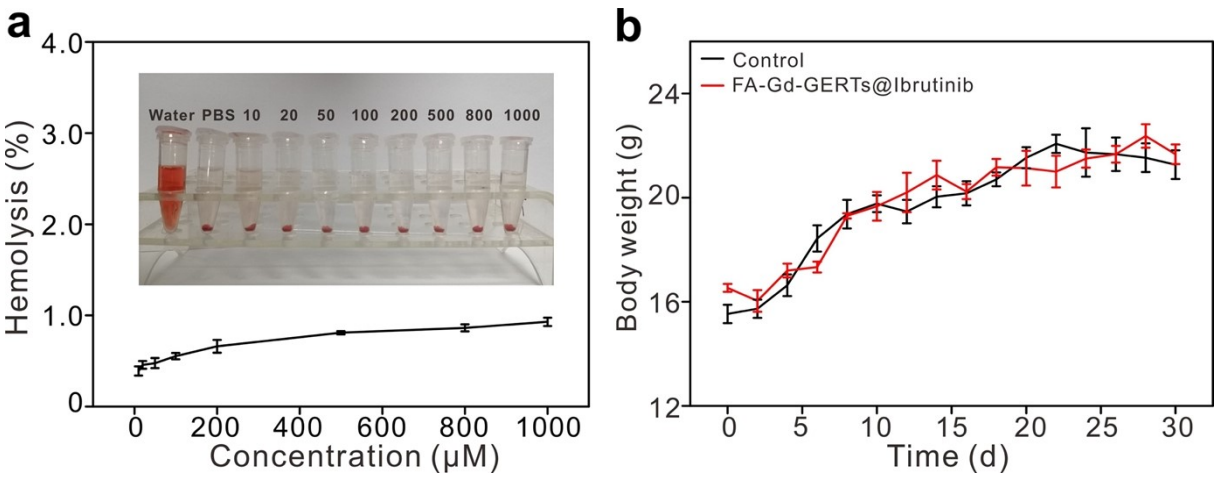

Fig. S12. (a) *In vitro* hemolysis assay. Percentage of hemolytic RBCs incubated with FA-Gd-GERTs@Ibrutinib of different concentrations for 6 h, using deionized water (+) and PBS (−) as positive and negative controls, respectively. Inset: photograph of direct observations of hemolysis. (b) Body weight cures of mice for FA-Gd-GERTs@Ibrutinib and control groups for 30 days.